Keywords: Minkowski plane, geometry, pi, perimeter, Banach spaces

π_B IN ASYMMETRIC MINKOWSKI NORMED SPACES

GORKA GUARDIOLA MÚZQUIZ

ABSTRACT. We extend the classical results of Stanisław Gołab, on the values of pi in arbitrary normed planes, to asymmetric norms where the unit ball has one axis of symmetry. First, we characterize the values of π_B for different families of polygons as unit ball B. Then we prove that $\pi_B \geq 3$, and can take all possible values and is not bounded in such spaces.

1. Introduction

Starting with an appropriately chosen set for the unit ball, B, a Minkowski functional can be defined to act as a norm. That norm is completely characterized by the geometric properties of the set B. In the constructed Banach space, the value of π_B, the half-perimeter of the unit ball B measured by its norm is not $\pi = 3.1415\ldots$

Classical results by Gołab state that for any norm in $\mathbb{R}^2$, $\pi_B \in [3, 4]$ and that for norms that have a quarter-turn symmetry, $\pi_B \geq \pi$. The papers [1, 2, 3, 4, 5], prove this and other facts about π_B for different norms in $\mathbb{R}^2$. Under certain conditions (a unit ball with one axis of symmetry), a definition of the measurement of the perimeter can be made for asymmetric Minkowski normed spaces, where the unit ball is not centrally symmetric. For these spaces, we calculate π_B for different sets acting as unit ball, B, (e.g. all the regular polygons), and find that, in general, $\pi_B \in [3, \infty)$, taking all possible values.

In this section and the next one, some of the results we state are from [6] and [5] and cited without proof. In Section 2 we introduce asymmetric norms and the conditions for which the perimeter (and thus π_B) is well defined. In Section 3 we characterize all the norms (including asymmetric norms) for which the unit ball B is a convex regular polygon. In Section 4 we calculate π_B for some convex polygons, with different centers. In Section 5 we find the bounds for π_B for any asymmetric norm.

Along the paper, $\mathbb{R}$ are the real numbers, and $\mathbb{R}^+$ are the strictly positive real numbers $x > 0$. We use $B_1 \subset B_2$ like [6] to mean what other authors write as $B_1 \subseteq B_2$, that is, the subset inclusions we consider are never strict.

B is the unit Ball, $B := \{x \in X : ||x|| \leq 1\}$, its interior $B^o := \{x \in X : ||x|| < 1\}$, and its boundary $\partial B := \{x \in X : ||x|| = 1\}$.

We will denote π the half-perimeter of the unit ball of the Euclidean norm, i.e. $\pi = 3.14\ldots$ and π_B with a subindex B the half-perimeter of the unit ball of a norm specified by B.

Definition 1.1. A norm on a real linear space X (i.e. a finite dimensional real vector space) is a mapping $||\cdot||$ from X into $\mathbb{R}^+$ that satisfies the following axioms:

(i) $||x|| \geq 0$ with equality if and only if $x = 0$,
(ii) $||\alpha x|| = |\alpha|||x||$ $(\alpha \in \mathbb{R})$,

Date: November 11, 2025.

(iii) $||x+y|| \leq ||x|| + ||y||$.

Definition 1.2. A set, B, is convex if it contains all the straight line segments connecting two points, $x, y \in B$.

Definition 1.3. A set is centrally symmetric if, given a point x contained in the set, its antipodal point, $-x$, is also contained in the set.

Proposition 1.4. If B is a centrally symmetric convex set in X such that each line through 0 meets B in a non-trivial, closed, bounded segment then $||\cdot||_B$ is a norm in X where $||\cdot||_B$ comes from the next definition, given B meets the properties stated above (proposition 1.1.8 in [6]).

Definition 1.5. The functional $||\cdot||_B$, called the *Minkowski functional of* B is defined by $||x||_B := inf\{\xi \in \mathbb{R}^+ : x \in \xi B\}$, or, equivalently, given that B is closed and the space is complete: $||x||_B := \frac{1}{sup\{\xi \in \mathbb{R}^+ : \xi x \in B\}}$.

Theorem 1.6. *The unit ball in a Minkowski space given by a linear space and a norm, $(X, ||\cdot||_B)$ is centrally symmetric and convex (theorem 1.1.6 in* [6]*).*

Definition 1.7. The perimeter of a polygon $\mathcal{P} := [x_0, x_1, \ldots, x_n]$, with $x_i \in \mathbb{R}^2$ with respect to a norm $||\cdot||_B$ is $\mu_B(P) := \sum_{i=1}^{n} ||x_i - x_{i-1}||_B$.

Given a curve $c := \{x : x = \phi(t)\, \alpha \leq t \leq \beta\}$ and partitions of $[\alpha, \beta]$ given by $\alpha = t_0 < t_1 < \cdots < t_n = \beta$ we may consider a family of polygons, one for each partition $\mathcal{P}_a = [\phi(t_0), \phi(t_1), \ldots, \phi(t_n)]$. Because of the triangle inequality, the perimeters of the polygons increase as the partition is refined. A curve is *rectifiable* if the perimeter of each of the polygons $\mathcal{P}_a$ associated to a partition of the curve is bounded from above.

Definition 1.8. The length of a rectifiable curve $c \in \mathbb{R}^2$ with an inscribed family of polygons as described above $\mathcal{P}_a$ is defined to be: $\mu_B(c) := sup_a\{\mu_B(\mathcal{P}_a)\}$.

Proposition 1.9. If a convex curve c_1 is inscribed inside another convex curve c_2, its measure is smaller, i.e. $\mu_B(c_1) \leq \mu_B(c_2)$ (Proposition 4.3.4 in [6]).

From [5] we have the following:

Proposition 1.10. The boundary of a convex set, $c \in \mathbb{R}^2$, is a convex path. It is a convex curve, is rectifiable and, thus, has finite measure, i.e. $\mu_B(c) \in [0, \infty)$.

By proposition 1.10, the length of the unit ball boundary ∂B, which is a convex path by 1.6, is finite, i.e. $\mu_B(\partial B) \geq k$, $k \in \mathbb{R}$. Also $k > 0$ because of the other conditions for the set B in Proposition 1.4.

2. Asymmetric Minkowski normed spaces

We are interested in *asymmetric* norms. That means we relax axiom (ii) in 1.1.

Definition 2.1. An asymmetric norm $||x||$ has the following properties.

(i) $||x|| \geq 0$ with equality if and only if $x = x_0$,
(ii) $||\alpha x|| = \alpha ||x||$ $(\alpha \in \mathbb{R}^+)$,
(iii) $||x+y|| \leq ||x|| + ||y||$.

All the properties are the same of a norm, except $||x||$ and $||-x||$ may be different. The origin is not 0 but an arbitrary $x_0 \in B^o$.

Proposition 2.2. If B is a convex set in X such that each line through x_0 meets B in a non-trivial, closed, bounded segment (i.e. a segment of positive bounded length with edges different than the origin), then $||\cdot||_B$ is a asymmetric norm in X where $||\cdot||_B$ comes from the same Minkowski functional defined by 1.5.

Note that we have dropped the condition of central symmetry in B. We will prove Proposition 2.2 for the appropiate off-center Minkowski functional next. In the original proposition 1.4, the center from which to calculate the norm was defined implicitly. As the set was centrally symmetric around 0, we could use that center to define the Minkowski functional. In the asymmetric case, though, there is more freedom in the choice of center. Any center $x_0 \in B^o$ is equally valid:

Definition 2.3. The functional $||\cdot||_{B,x_0}$, called the *offset Minkowski functional of B at x_0* is defined by $||x||_{B,x_0} := inf\{\xi \in \mathbb{R}^+ : x \in \xi(B - x_0)\}$ or, equivalently, $||x||_{B,x_0} := \frac{1}{sup\{\xi\in\mathbb{R}^+ : \xi x\in(B-x_0)\}}$, where $B - x_0$ means: "the set composed of all elements $x - x_0$ where $x \in B$".

Theorem 2.4. *An asymmetric norm defined by its Minkowski functional in 2.3 meets the properties stated in Definition 2.1.*

Proof. Linearity (i) comes trivially from the definition of the functional. Non-negativity (ii) comes from the fact that $x_0 \in B^o$ and that each line through x_0 meets B in a non-trivial closed bounded segment. We will use $||x||_{B,x_0}$ or $||x||_B$ when the choice of center is obvious or does not matter.

The triangle inequality (iii) is met because of the convexity of the unit ball (we can just reuse the classic proof): Given the definition in 1.5, $||x||_B := \frac{1}{sup\{\xi\in\mathbb{R}^+ : \xi x\in B\}}$, a vector x is inside the unit ball, i.e. $x \in B$, if and only if $||x||_B \leq 1$. For a convex set B, given two points, x and y, any vector $z = (1 - t)x + ty$, where $t \in [0, 1]$ then $z \in B$ (this is the standard definition of a convex set). This means that $\frac{x+y}{||x||_B+||y||_B} = \left(\frac{x}{||x||_B}\right)\frac{||x||_B}{||x||_B+||y||_B} + \left(\frac{y}{||y||_B}\right)\frac{||y||_B}{||y||_B+||y||_B} = t\frac{x}{||x||_B} + (1 - t)\frac{y}{||y||_B}$, where $t = \frac{||x||_B}{||x||_B+||y||_B}$. Clearly, $\frac{x+y}{||x||_B+||y||_B} \in B$, so $\frac{||x+y||_B}{||x||_B+||y||_B} \leq 1$ and $||x+y||_B \leq ||x||_B + ||y||_B$. $\square$

When some families of sets are used as unit ball (like regular polygons), there is an obvious choice of center. In other cases (or even for regular polygons), different centers can be defined. We will try to tackle this question with as much generality as possible (in $\mathbb{R}^2$).

Another important obstacle when dealing with asymmetric norms in $\mathbb{R}^2$ is that the definition of perimeter in Definition 1.7 is not unique and depends on the choice of direction for each of the sides. In general $\sum_{i=1}^{n} ||x_i - x_{i-1}||_B \neq \sum_{i=1}^{n} ||x_{i-1} - x_i||_B$. Even worse than two possible measurements of the perimeter of a polygon, (clockwise or counterclockwise) we can obtain, potentially, 2^n different measurements for the perimeter: two values per side, one per orientation. Clearly, some additional conditions must be met for the half-perimeter (i.e. π_B) to be unique.

First, we give some definitions and then we will state the conditions:

Definition 2.5. The counterclockwise perimeter of a polygon $\mathcal{P} := [x_0, x_1, \ldots, x_n]$, $x_i \in \mathbb{R}^2$ with respect to a possibly asymmetric norm $||\cdot||_B$ for $\mathbb{R}^2$ is $\overset{\circlearrowleft}{\mu}_B(P) := \sum_{i=1}^{n} ||x_i - x_{i-1}||_B$ where the enumeration of vertices of the polygon is ordered counterclockwise.

Definition 2.6. With the same enumeration, but different order, the clockwise perimeter is: $\overset{\circlearrowright}{\mu}_B(P) := \sum_{i=1}^{n} ||x_{i-1} - x_i||_B$. where the enumeration of vertices of the polygon is ordered clockwise.

Definition 2.7. The maximum perimeter of a polygon $\mathcal{P} := [x_0, x_1, \ldots, x_n]$, $x_i \in \mathbb{R}^2$ with respect to a possibly asymmetric norm $|| \cdot ||_B$ for $\mathbb{R}^2$ is $\overset{max}{\mu}_B(P) := \sum_{i=1}^{n} max\{||x_i - x_{i-1}||_B, ||x_{i-1} - x_i||_B\}$.

The maximum perimeter is equivalent to taking the perimeter with respect to a (symmetric) norm obtained from the symmetrization of B. $\overset{max}{\mu}_B(P) = \mu_{B_{si}}(P)$ where $B_{si} = B \cap -B$ and $-B$ denotes the set $-B := \{-x : x \in B\}$. Note that a smaller B radius means a bigger measurement of the corresponding vector. B_{si} is the intersection of two convex sets (which is itself convex), so it meets all the conditions to be the unit ball of an asymmetric norm as stated in Proposition 2.2. B_{si}, is also centrally symmetric, from its definition, so $|| \cdot ||_{B_{si}}$ is a norm.

Definition 2.8. The minimum perimeter of a polygon $\mathcal{P} := [x_0, x_1, \ldots, x_n]$ with respect to a possibly asymmetric norm $||\cdot||_B$ for $\mathbb{R}^2$ is $\overset{min}{\mu}_B(P) := \sum_{i=1}^{n} min\{||x_i - x_{i-1}||_B, ||x_{i-1} - x_i||_B\}$.

Unfortunately the union of convex sets is not necessarily convex, so $B_{su} = B \cup -B$ is not convex so $|| \cdot ||_{B_{su}}$ may not be a norm. An example of this is a triangle. The union of the triangle and its reflection is a star polygon (an hexagram), non-convex. The convex hull of a set A, $conv(A)$, is the minimum convex set containing it. The smallest symmetric ball containing B_{su} is its convex hull $conv(B_{su})$. Note that if the unit ball of a norm (asymmetric or not) is contained inside another $B_1 \subset B_2$, then $||v||_{B_2} \leq ||v||_{B_1}$ from the definition of the Minkowski functional and the triangle inequality.

From all these definitions, it is evident that:

$$\mu_{conv(B_{su})}(P) \leq \overset{min}{\mu}_B(P) \leq \overset{\circlearrowleft}{\mu}_B(P) \leq \overset{max}{\mu}_B(P) = \mu_{B_{si}}(P) \tag{2.1}$$

and

$$\mu_{conv(B_{su})}(P) \leq \overset{min}{\mu}_B(P) \leq \overset{\circlearrowright}{\mu}_B(P) \leq \overset{max}{\mu}_B(P) = \mu_{B_{si}}(P). \tag{2.2}$$

For a symmetric norm $\overset{max}{\mu}_B(P) = \overset{min}{\mu}_B(P)$ so $\overset{\circlearrowleft}{\mu}_B(P) = \overset{\circlearrowright}{\mu}_B(P)$. For a strictly asymmetric norm (an asymmetric norm with a not centrally symmetric unit ball[1]) $\overset{min}{\mu}_B(P) \leq \overset{max}{\mu}_B(P)$. Note that, while $\overset{min}{\mu}_B(P) = \overset{max}{\mu}_B(P)$ implies $\overset{\circlearrowleft}{\mu}_B(P) = \overset{\circlearrowright}{\mu}_B(P)$, the converse is not true. We want to impose the minimum conditions necessary, so that $\overset{\circlearrowleft}{\mu}_B(P) = \overset{\circlearrowright}{\mu}_B(P)$.

Under what conditions is $\overset{\circlearrowleft}{\mu}_B(P) = \overset{\circlearrowright}{\mu}_B(P)$? Just one condition is sufficient: a single axis of symmetry shared by the unit ball and the polygon whose perimeter is being measured. Under this condition, each side (or fragment of a side if the axis of symmetry cuts a side in two), can be paired with its symmetric, so each side measured clockwise will be transposed for the same side when measured counterclockwise but with its symmetric radius of the same length as depicted in Figure 1.

[1]Remember all norms are, by definition an asymmetric norms which have to meet a subset of the conditions met by a norm.

If we want to measure a convex path C, and it shares the same axis of symmetry, we can rectify it with polygon refinements, P_i, with a growing number of sides. The refinements grow as more points are added because of the triangle inequality so $\mu_B(P_i) \geq \mu_B(P_j)$ when $i \geq j$, but as it is bounded because it is a convex path, the length of the refinements converges. We will denote the limit of the measure $\mu_B(C) = sup\,\mu_B(P_i) = sup\,\overset{\circlearrowleft}{\mu}_B(P_i) = sup\,\overset{\circlearrowright}{\mu}_B(P_i)$.

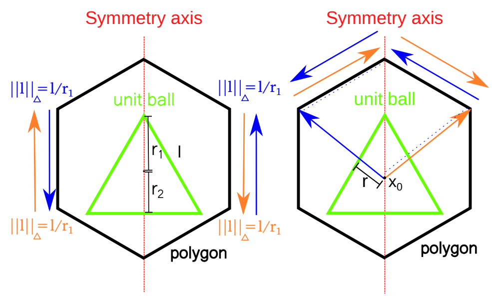

Figure 1. Ball and polygon with an axis of symmetry

2.1. **Radon norms.** From [5] we introduce the following definitions:

Definition 2.9. Let X be a norm on $\mathbb{R}^n$ and consider two nonzero vectors $x, y \in \mathbb{R}^n$. We will say y is *Birkhoff orthogonal* to x, written $y \vdash_X x$, if $||x + ty||_X \geq ||x||_X$ for all $t \in \mathbb{R}$. This is equivalent to stating that the line $\{x + ty : t \in \mathbb{R}\}$ is "tangent" to the ball of radius $||x||_X$ meaning it intersects the ∂B. but not B^o.

For a Euclidean norm we have $y \vdash_X x$, if and only if $\langle x, y\rangle = 0$, so $\vdash_X$ is symmetric. This symmetry does not hold in general: $y \vdash_X x \not\Rightarrow x \vdash_X y$.

Definition 2.10. A norm $X \in \mathbb{R}^2$ is said to be *Radon* if the relation $\vdash_X$ is symmetric[2].

This is Theorem 4.7 in [5] (see [4],[7], [8] and [9] for more details):

Definition 2.11. Lets call the set of all Radon norms with a unit ball B, $\mathcal{R}$. Then $\pi_B \in [3, \pi]$, with $\pi_B = \pi$, if and only if B is an ellipse (i.e. it belongs to the Euclidean norm under linear isomorphisms, see [5]).

3. Regular convex polygons

All regular convex polygons have at least two axes of symmetry [10], so they meet the conditions stated above (when acting both as unit ball and as polygon being measured, i.e. to find π_P) so that $\overset{\circlearrowleft}{\mu}_P(P) = \overset{\circlearrowright}{\mu}_P(P)$, which we will denote simply $\mu_P(P)$, so $\pi_P = \frac{\mu_P(P)}{2}$. Note that polygons with an even number of sides have central symmetry [10] and as such the Minkowski functional is a norm. Polygons with an odd number of sides are not centrally symmetric so they induce a Minkowski functional which is an asymmetric norm. For any regular convex polygon we can use as center the point where all the axes of symmetry meet. Even more, each side

[2]Note that Radon norms are special in two dimensions. In three or more dimensions, a norm is Radon if and only if it is Euclidean (see [5]), whereas in two dimensions, they can be non-Euclidean.

is measured, because of the rotational symmetries [10] both of the unit ball, and the polygon being measured (both are the same) with equal radius, so their measures are equal. The half-perimeter of a regular convex polygon is then $\pi_B = \frac{\mu_B(P)}{2} = \frac{\sum_1^n ||l_i||_B}{2} = \frac{n||l_1||_B}{2}$.

We will denote it as π_n or, for some special cases like, when B is a regular triangle, as $\pi_\triangle$, so we will use indistinctively π_B, π_3 or $\pi_\triangle$.

To illustrate the procedure, let's start with the regular triangle, $\pi_\triangle = \frac{\mu_\triangle(\triangle)}{2}$.

We will measure the perimeter anti-clockwise. We apply definition (1.5) to calculate $||l_n||_\triangle$. For each side, we translate it to the origin to find the radius which applies to it (r as can be seen in Figure 2). Because the triangle is the unit ball $r = 1$. In Figure 2 we measure two sides (as an example, as stated before, with one is enough, the rest are the same). From the geometric construction in Figure 2, $l_1 = 3$, so $\pi_\triangle = \frac{\mu_\triangle(\triangle)}{2} = 3\frac{||l_1||_\triangle}{2} = \frac{9}{2} = 4.5$. Note that scaling the unit ball does not change its measure, because if the length of the sides is scaled by a, so is the radius by which they are being measured, by similarity, and $||l||_b = \frac{||al||}{||ar||} = \frac{||l||}{||r||}$, so $||l_b||$ is unchanged, where $||x||$ without subindex denotes the regular Euclidean norm.[3]

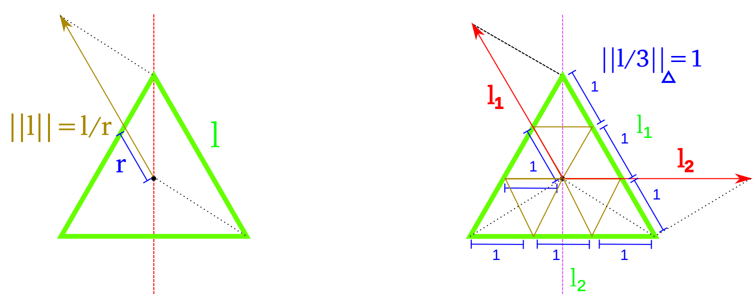

FIGURE 2. Triangle as unit ball

Note that this value is outside of Gołab's theorem range [11] for symmetric two dimensional norms (i.e. $\pi_{B_{sym}} \in [3, 4]$).

When measuring the perimeter of a regular convex polygon (with itself as unit ball), the measurements defined in 2.5, 2.6, 2.7 and 2.8 are the same so $max\{||l_1||_P, ||-l_1||_P\} = ||l_1||_P = ||-l_1||_P$ and $min\{||l_1||_P, ||-l_1||_P\} = ||l_1||_P = ||-l_1||_P$, and $\overset{min}{\mu}_P(P) = \overset{\circlearrowleft}{\mu}_P(P) = \overset{\circlearrowright}{\mu}_P(P) = \overset{max}{\mu}_P(P)$: any of these measurements would give the same value of π_P.

Just applying some trigonometry and definition (1.5), the half-perimeter of any regular polygon can be calculated[4], as seen in Figure 3.

In Figure 4 and Table 1 we present the values of the half-perimeter for different convex regular polygons. A general formula can be calculated for *all* the convex regular polygons. In [12] a formula for the Minkowski functional of a polygon is

[3]This can be generalized to a linear isomorphism, when the polygon defines a (symmetric) norm see [5]. The same can be done for linear isomorphisms with positive eigenvalues for asymmetric norms.

[4]Note that the apothem (or radius of the inscribed circle) is: $a_n = \frac{l}{2\tan(\frac{\pi}{n})}$

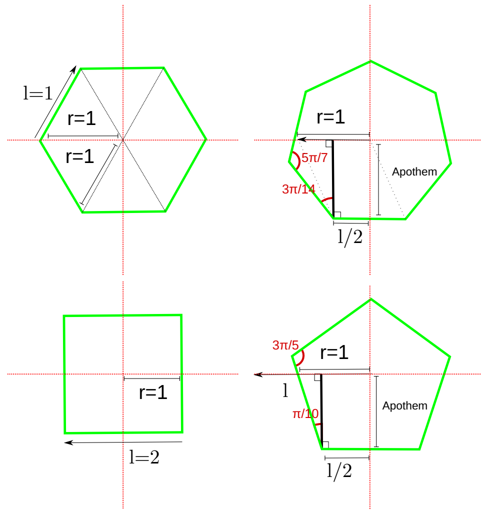

FIGURE 3. Constructions to calculate the measure of a side

Number of sides	π_n	π_n
3	$9/2$	$9/2$
4	4	4
5	3.454915028125262879488532914085904706	$\frac{5(5-\sqrt{5})}{4}$
6	3	3
7	3.286503763716470257372386327536920665	$28\sin^2(\frac{\pi}{7})\sin(\frac{3\pi}{14})$
8	3.313708498984760390413509793677584628	$8\sqrt{2}-8$
9	3.225966377139231493977618069073666967	$2+2\cos(2\frac{\pi}{9})$
10	3.090169943749474241022934171828190589	$\frac{5+5\sqrt{5}}{2}$

TABLE 1. Values of π_n vs. number of sides

found.

$$||r||_{B_n} = max_i\{\langle r, a_{(m,n)}\rangle, i \in 1,\dots,m\}, \tag{3.1}$$

where $\langle r, a_{(m,n)}\rangle$ denotes the inner product of the vector $r=(x,y)$ and $a_{(m,n)} = \frac{1}{\cos\left(\frac{\pi}{n}\right)}\left(\cos\left((2m-1)\frac{\pi}{n}\right), \sin\left((2m-1)\frac{\pi}{n}\right)\right)$.

The side of a polygon is the vector $l = (\cos(2\pi/n)-1, \sin(2\pi/n))$, so

$$||l||_n = max_m\left\{\frac{\left(\cos\left(\frac{2\pi}{n}\right)-1\right)\cos\left((2m-1)\frac{\pi}{n}\right)+\sin\left(\frac{2\pi}{n}\right)\sin\left((2m-1)\frac{\pi}{n}\right)\big)}{\cos\left(\frac{\pi}{n}\right)}, m\in 1,\dots,n\right\},$$

and its half-perimeter is, because of rotational symmetry, $\pi_n = \frac{n||l||_n}{2}$, so

$$\pi_n = n\frac{max_m\left\{\left(\left(\cos\left(\frac{2\pi}{n}\right)-1\right)\cos\left((2m-1)\frac{\pi}{n}\right)\right)+\sin\left(\frac{2\pi}{n}\right)\sin\left((2m-1)\frac{\pi}{n}\right)\right), m\in 1,\dots,n\right\}}{2\cos\left(\frac{\pi}{n}\right)}.$$

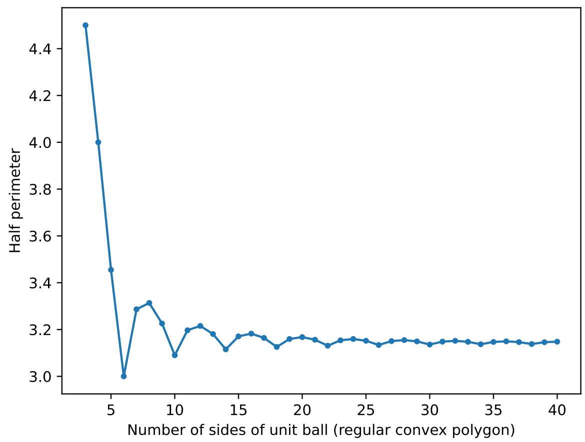

FIGURE 4. Values of π_{B_n} vs. number of sides

Applying product-to-sum trigonometric identities:
(3.2)
$$\pi_n = \frac{n}{2\cos\left(\frac{\pi}{n}\right)} max_m \left\{ \left(\cos\left(\frac{3\pi}{n} - \frac{2m\pi}{n}\right) - \cos\left(\frac{\pi}{n} - \frac{2m\pi}{n}\right)\right), m \in 1, \ldots, n \right\}.$$

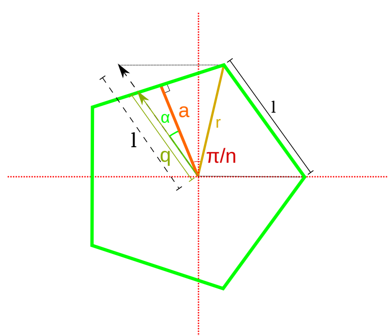

FIGURE 5. General construction to measure the side

We can simplify this expression further. First we need to show where the expression comes from. Figure 5 depicts the elements necessary for an example pentagon. If, in that figure $r = 1$, then $||l||_n = \frac{||l||}{||q||}$ and $||q|| = \frac{\cos(\pi/n)}{\cos(\alpha)}$. So finally, $||l||_n = \frac{||l||\cos(\alpha)}{\cos(\pi/n)}$. If we take u to be the unit vector $u = \frac{a}{||a||}$, then $\langle u, l\rangle = ||l||cos(\alpha)$, but u for the side of index m is: $u_{m,n} = \left(\cos\left(\frac{m2\pi}{n} - \frac{\pi}{n}\right), \sin\left(\frac{m2\pi}{n} - \frac{\pi}{n}\right)\right)$. so $||l||_n = \frac{||l||\cos(\alpha)}{\cos(\pi/n)} = \frac{\langle u_{m,n}, l\rangle}{\cos(\pi/n)}$, but $a_{m,n} = \frac{u_{m,n}}{\cos(\pi/n)}$, so we recover (3.1). The maximum in the equation is there to find which side is intersected by the vector (which when calculating the half-perimeter is also a side of the polygon) being measured by the functional. We can calculate more precisely which side is intersected. It depends on the number of sides subtended by the angle β in Figure 6. First we find the values of the different angles on the figure. The inside angle of a regular convex polygon of n sides is: $\gamma = \frac{(n-2)\pi}{n}$. Also, the angle δ is [10]: $\delta = \frac{2\pi}{n}$. Finally, the number of subtended sides $m = \left\lceil \frac{\beta}{\delta} \right\rceil = \left\lceil \frac{\pi - \gamma/2}{\delta} \right\rceil = \left\lceil \frac{\pi - \frac{(n-2)\pi}{2n}}{\frac{2\pi}{n}} \right\rceil = \left\lceil \frac{n+2}{4} \right\rceil = \left\lfloor \frac{n+5}{4} \right\rfloor$.

Substituting in (3.2) and simplifying:
(3.3)

$$\pi_n = \frac{n}{2\cos\left(\frac{\pi}{n}\right)} \left(\cos\left(\frac{\pi}{n} \left(-1 + 2\left\lfloor \frac{n+1}{4} \right\rfloor \right) \right) - \cos\left(\frac{\pi}{n} \left(1 + 2\left\lfloor \frac{n+1}{4} \right\rfloor \right) \right) \right).$$

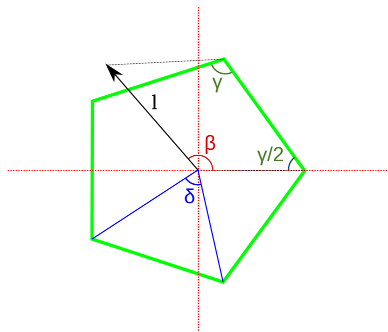

FIGURE 6. Sides subtended by β

The limit when the number of sides n tends to ∞ is π as expected. To obtain it, note that, in the limit, we can ignore the floor function as it is asymptotically negligible: $\lim_{n\to\infty} \pi_n = \lim_{n\to\infty} \frac{n}{2\cos\left(\frac{\pi}{n+1}\right)} \left(\cos\left(\frac{\pi}{n+1} \left(-1 + n/2 \right) \right) - \cos\left(\frac{\pi}{n} \left(1 + n/2 \right) \right) \right) =$ $\lim_{n\to\infty} \frac{n}{2} \left(\sin\left(\frac{\pi}{n}\right) + \sin\left(\frac{\pi}{n}\right) \right)$, so $= \lim_{n\to\infty} \frac{n}{2} \left(\frac{\pi}{n} + \frac{\pi}{n} \right) = \pi$.

Note also that π_n as a function of n oscillates with period 4 as seen in Figure 4. The function behaves as a convex function until an extra side is subtended by the angle β. Each time this happens, it reaches a minimum and bounces back.

Number of sides	π_n
$[3, 6]$	$\frac{n}{2\cos\left(\frac{\pi}{n}\right)} \left(\cos\left(\frac{\pi}{n}\right) - \cos\left(\frac{3\pi}{n}\right) \right)$
$[7, 10]$	$\frac{n}{2\cos\left(\frac{\pi}{n}\right)} \left(\cos\left(\frac{3\pi}{n}\right) - \cos\left(\frac{5\pi}{n}\right) \right)$
$[11, 14]$	$\frac{n}{2\cos\left(\frac{\pi}{n}\right)} \left(\cos\left(\frac{5\pi}{n}\right) - \cos\left(\frac{7\pi}{n}\right) \right)$
$[15, 18]$	$\frac{n}{2\cos\left(\frac{\pi}{n}\right)} \left(\cos\left(\frac{7\pi}{n}\right) - \cos\left(\frac{9\pi}{n}\right) \right)$

TABLE 2. Values of π_n vs. number of sides

When $n = 6$ the radius is equal to the side as can be seen in Figure 3 and the subtended number of sides is a round number. The cosine in the right side of the expression in table 2, $\cos\left(\frac{3\pi}{n}\right)$ is zero[5].

[5]Something similar happens when $n = 10, 14\ldots$ This is the reason these polygons induce Radon measures as we will see later.

For n multiple of 4, $\left\lfloor \frac{n+1}{4} \right\rfloor = \frac{n}{4}$, and equation (3.3) can be simplified $\pi_n = \frac{n}{2\cos\left(\frac{\pi}{n}\right)}\left(\cos\left(\frac{\pi}{n}\left(-1+2\frac{n}{4}\right)\right) - \cos\left(\frac{\pi}{n}\left(1+2\frac{n}{4}\right)\right)\right)$, so:

$$\pi_n = n\tan\left(\frac{\pi}{n}\right) \tag{3.4}$$

For n an exponent of 2, $n = 2^m$ the paper [13] gives a formula for $\sin\left(\frac{\pi}{2^m}\right) = \frac{1}{2}\sqrt{2-\underbrace{\sqrt{2+\sqrt{2}}\cdots}_{\text{m-2 times}}}$ and $\cos\left(\frac{\pi}{2^m}\right) = \frac{1}{2}\sqrt{2+\underbrace{\sqrt{2+\sqrt{2}}\cdots}_{\text{m-2 times}}}$, so, for $m \geq 2$ so $\pi_{2^m} = 2^m\frac{\sqrt{2-\overbrace{\sqrt{2+\sqrt{2}}\cdots}^{\text{m-2 times}}}}{\sqrt{2+\underbrace{\sqrt{2+\sqrt{2}}\cdots}_{\text{m-2 times}}}}$. From this we can obtain a Viète-like formula:

$$\pi = \lim_{m\to\infty} 2^m\frac{\sqrt{2-\overbrace{\sqrt{2+\sqrt{2}}\cdots}^{\text{m-2 times}}}}{\sqrt{2+\underbrace{\sqrt{2+\sqrt{2}}\cdots}_{\text{m-2 times}}}}. \tag{3.5}$$

3.1. **Simpler expression.** We start with equation (3.3) and we write $n = 4m+k$, where $m \in \{1,2,\ldots\}$ and $k \in \{0,1,2,3\}$:

$$\pi_n = \frac{n}{2\cos\left(\frac{\pi}{n}\right)}\left(\cos\left(\frac{\pi}{n}\left(-1+2\left\lfloor\frac{4m+k+1}{4}\right\rfloor\right)\right) - \cos\left(\frac{\pi}{n}\left(1+2\left\lfloor\frac{4m+k+1}{4}\right\rfloor\right)\right)\right) =$$
$$\frac{n}{2\cos\left(\frac{\pi}{n}\right)}\left(\cos\left(\frac{\pi}{n}\left(-1+2m+2\left\lfloor\frac{k+1}{4}\right\rfloor\right)\right) - \cos\left(\frac{\pi}{n}\left(1+2m+2\left\lfloor\frac{k+1}{4}\right\rfloor\right)\right)\right).$$

Applying trigonometric angle sum identities:

$$\pi_n = \frac{n}{2\cos\left(\frac{\pi}{n}\right)}2\sin\left(\frac{2\pi}{n}\left(m+\left\lfloor\frac{k+1}{4}\right\rfloor\right)\right)sin\left(\frac{\pi}{n}\right) = n\tan\left(\frac{\pi}{n}\right)\sin\left(\frac{2\pi}{n}\left(m+\left\lfloor\frac{k+1}{4}\right\rfloor\right)\right).$$

When $n = 4m$, $k = 0$, the right side equals $\sin(\pi/2) = 1$ and we recover equation (3.4). We have three other cases, $k = 1$, $k = 2$ and $k = 3$. For the cases $k \in \{1,2\}$, $\left\lfloor\frac{k+1}{4}\right\rfloor = 0$, so $\sin(\frac{2\pi}{n}(m+\lfloor\frac{k+1}{4}\rfloor)) = \sin\left(\frac{2\pi}{n}m\right)$, but $m = \frac{(n-k)}{4}$, so $\sin(\frac{2\pi}{n}m) = \sin(\frac{2\pi(n-k)}{4n}) = \sin(\frac{\pi}{2}-\frac{2\pi k}{4n}) = \cos(\frac{\pi k}{2n})$.

For the case $k = 3$, $\left\lfloor\frac{k+1}{4}\right\rfloor = 1$, so following a similar reasoning, $\sin(\frac{2\pi}{n}(m+\lfloor\frac{k+1}{4}\rfloor)) = \cos(\frac{\pi}{2n})$.

$$\pi_n = \begin{cases} n\tan\left(\frac{\pi}{n}\right) & n = 4m \\ n\tan\left(\frac{\pi}{n}\right)\cos(\frac{\pi}{2n}) & n = 4m+1,\ n = 4m+3 \\ n\tan\left(\frac{\pi}{n}\right)\cos(\frac{\pi}{n}) = n\sin\left(\frac{\pi}{n}\right) & n = 4m+2. \end{cases} \tag{3.6}$$

Note that the condition for the second case can be written as $n = 2m+1$.

Seeing that the value of π_n is a piecewise function, we can separate the plot in Figure 4 for each of the cases in (3.6) as can be see in Figure 7. This clarifies the plot and gives us the intuition to calculate bounds later.

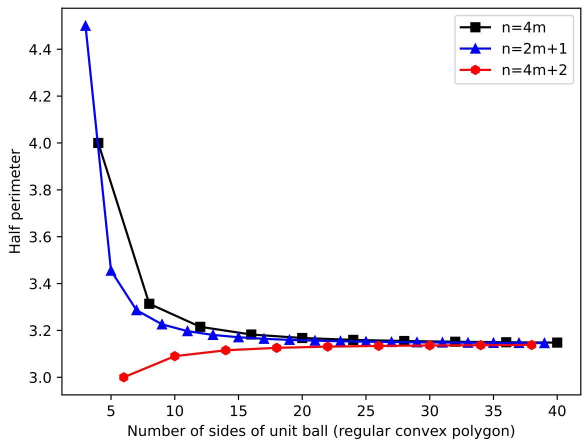

FIGURE 7. Values of π_{B_n} vs. number of sides

3.2. **Beraha numbers.** The nth Beraha number or Beraha constant [14] is given by $B_n = 2 + 2\cos\left(\frac{2\pi}{n}\right) = 4\cos\left(\frac{\pi}{n}\right)^2$.

The sequence[6] is shown in Table 3,

n	B_n
1	4
2	0
3	1
4	2
5	$\phi + 1$
6	3
7	$2 + 2\cos(\frac{2\pi}{7}) = S$
8	$2 + \sqrt{2}$
9	$2 + 2\cos(\frac{2\pi}{9})$
10	$\phi + 2$,

TABLE 3. Beraha numbers B_n

There are simple algebraic expressions of π_n in terms of Beraha constants.

[6] ϕ is the golden ratio, $\phi = \frac{1+\sqrt{5}}{2}$ and S is the silver constant.

When $n = 4m$, applying the pythagorean identity: $\pi_n = n\tan\left(\frac{\pi}{n}\right) = n\frac{\sin\left(\frac{\pi}{n}\right)}{\cos\left(\frac{\pi}{n}\right)} = n\frac{\sqrt{1-\cos\left(\frac{\pi}{n}\right)^2}}{\cos\left(\frac{\pi}{n}\right)}$. Applying the half angle identity, $\cos(a/2) = \sqrt{\frac{1+\cos(2a)}{a}}$ and simplifying, $\pi_n = n\sqrt{\frac{1-\cos(\frac{2\pi}{n})}{1+\cos(\frac{2\pi}{n})}} = n\sqrt{\frac{4-B_n}{B_n}}$.

Applying the half angle identity to the extra terms for the other cases: $\cos\left(\frac{\pi}{n}\right) = \sqrt{\frac{1+\cos\left(\frac{2\pi}{n}\right)}{2}} = \sqrt{\frac{B_n}{4}}$ and $\cos\left(\frac{\pi}{2n}\right) = \sqrt{\frac{1+\cos\left(\frac{\pi}{n}\right)}{2}} = \sqrt{\frac{1+\sqrt{\frac{B_n}{4}}}{2}}$.

Putting it all together:

$$\pi_n = \begin{cases} n\sqrt{\frac{4-B_n}{B_n}} & n = 4m \\ n\sqrt{\frac{4-B_n}{4B_n}}(2+\sqrt{B_n}) = n\sqrt{\frac{B_{2n}(4-B_n)}{4B_n}} & n = 4m+1,\ n = 4m+3 \\ n\sqrt{\frac{4-B_n}{4}} & n = 4m+2. \end{cases}$$

3.3. **Polygonal circle numbers.** In [12] so-called polygonal circle numbers were defined. They correspond to a different generalization of π from the one defined in this paper. They define circle numbers as $c_n = \alpha_B(B) = \int_B ||x||_B$, the area of the unit ball calculated radially pointing outside. They find them to be $c_n = \pi\frac{\sin\left(\frac{2\pi}{n}\right)}{\frac{2\pi}{n}}$.

Simplifying and applying the double integer identity, $\sin(2a) = 2\sin(a)\cos(a)$, $c_n = \frac{n\sin(\frac{2\pi}{n})}{2} = n\sin\left(\frac{\pi}{n}\right)\cos\left(\frac{\pi}{n}\right)$.

We can write π_n as a function of c_n,

$$\pi_n = \begin{cases} c_n\frac{1}{(\cos(\frac{\pi}{n}))^2} & n = 4m \\ c_n\frac{\cos(\frac{\pi}{2n})}{(\cos(\frac{\pi}{n}))^2} & n = 4m+1,\ n = 4m+3 \\ c_n\frac{1}{\cos(\frac{\pi}{n})} & n = 4m+2. \end{cases} \tag{3.7}$$

3.4. **Apothem.** The radius of the inscribed circle or apothem [10] of a polygon of circumscribed circle of radius one is $r_n = 2\sin(\frac{\pi}{n})$.

$$\pi_n = \begin{cases} \frac{nr_n}{2\cos(\frac{\pi}{n})} & n = 4m \\ \frac{nr_n\cos(\frac{\pi}{2n})}{2\cos(\frac{\pi}{n})} & n = 4m+1,\ n = 4m+3 \\ \frac{nr_n}{2} & n = 4m+2. \end{cases} \tag{3.8}$$

3.5. **Bounds for π_n.**

Theorem 3.1. *The value of π_n is bounded:*

$$\pi_n \in \begin{cases} (\pi, 4] & \textit{when } n = 4m \\ (\pi, \frac{9}{2}) & \textit{when } n = 4m+1,\ n = 4m+3 \\ [3, \pi) & \textit{when } n = 4m+2. \end{cases} \tag{3.9}$$

Proof. We can find the maximum and minimum for π_n by analyzing equation (3.6).

We can start with the case $4m+2$. This case, $f(n) = n\sin\left(\frac{\pi}{n}\right)$, grows uniformly when $n \geq 3$. With the Taylor series, it is easy to see that the derivative is positive and the function increases monotonically. Taking into account $\sin\left(\frac{\pi}{n}\right) = \frac{\pi}{n} + O(1/n^3)$, and that $\pi_n = n\sin\left(\frac{\pi}{n}\right)$ then, the $\lim_{n\to\infty} \pi_n = \pi$. As it grows monotonically with n, it attains its mimimum on the value $\pi_6 = 3$, so $3 \leq \pi_{4m+2} \leq \pi$.

The case $n = 4m$, $g(n) = n\tan\left(\frac{\pi}{n}\right)$ decreases monotonically when $n >= 4$, because n increases but $\tan\left(\frac{\pi}{n}\right)$ decreases and the second term dominates as can be seen from the Taylor series. All the terms are positive, so for the derivative, all the terms are negative when $n > 0$.

The limit $\lim_{n\to\infty} \pi_n = \pi$ is the same as the last case divided by $\cos\left(\frac{\pi}{n}\right)$ which tends to 1, so the limit is still π. Because of this, it attains it maximum when $\pi_4 = 4$ so $4 \leq \pi_{4m} \leq \pi$.

Finally, the cases where n is odd also decrease uniformly. It can be seen as the case for $n = 4m+2$ but with a faster cosine, which is the term which dominated. The limit is still π because $\lim_{n\to\infty} \cos\left(\frac{\pi}{2n}\right) = 1$, so $\frac{9}{2} \geq \pi_{2k+1} \geq \pi$, where $k \geq 1$, with its maximum at $\pi_3 = \frac{9}{2}$.

$$\pi_n \in \begin{cases} (\pi, 4] & \text{when } n = 4m \\ (\pi, \frac{9}{2}) & \text{when } n = 4m+1,\ n = 4m+3 \\ [3, \pi) & \text{when } n = 4m+2. \end{cases} \tag{3.10}$$

□

Note that the first case, when the polygons have a number of sides $n = 4m$ defines a (symmetric) norm with quarter-turn symmetry, which is known to have $\pi_{4m} \geq \pi$ as is proven in [5].

The other family of convex regular polygons inducing (symmetric) norms, are the ones with number of sides $n = 4m+2$. As stated by the following theorem these norms belong to $\mathcal{R}$ (the set of norms coming from a linear isomorphism of a Radon norm), which by Theorem 2.11 have $\pi_{4m+2} \in [3, \pi)$, and they are the only ones in that range, so no other convex regular polygons can induce a norm in $\mathcal{R}$.

Theorem 3.2. *Norms with convex regular polygons of $n = 4m+2$ sides as unit ball are Radon.*

Proof. To prove that these polygons induce Radon norms, we can follow a similar proof than Example 4.6 in [5]. By Definition 2.9, we need to prove Birkhoff orthogonality to be symmetric. We only need to prove it for the boundary of the unit ball, ∂B. If we take a point w on an edge (or its opposite), it admits only one supporting line (one line $u + tw$ intersecting ∂B such that $||w + tu||_B \geq ||w||_B$): the side to which it belongs. Translating this line to the origin, we find two points, vertices, x_1 and x_2 for which $x_1 \vdash_X w$ and $x_2 \vdash_X w$. These vertices admit many supporting lines (of the kind $||x_n + tw||_B \geq ||x_n||_B$) depicted as a grey wedge in Figure 8. They intersect the 4 sides adjacent to the 2 vertices. The angle α depicted in the figure, is $\alpha = \frac{2\pi}{n}$ because the internal angle of a polygon is $\beta = \frac{(n-2)\pi}{n}$, so the angle of the wedges is $\alpha = \pi - \beta = \pi - \frac{(n-2)\pi}{n} = \frac{2\pi}{n}$.

Each of these two wedges, when translated to the origin, intersect with the original edge and no other, so $w \vdash_X x$. In other words, we have each $4 = 2 + 2$

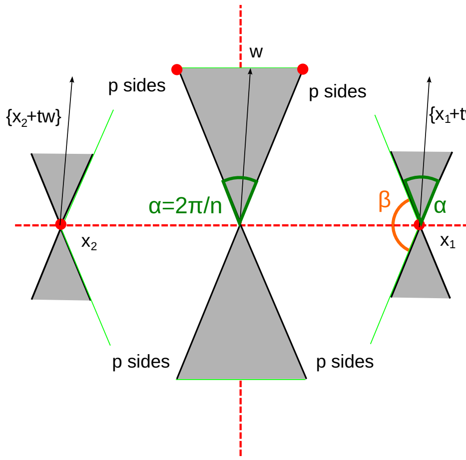

FIGURE 8. Polygon inducing radon norm

sides symmetrically Birkhoff orthogonal to the corresponding $2 = 1 + 1$ and $4p$, with $p \geq 0$, sides (the rest of the sides) which are not Birkhoff orthogonal in any direction with them. This makes in total $4 + 2 + 4p = 4m + 2$ sides. Another proof of this can be found in [15]. $\square$

The three families of polygons are then:

$$\pi_n \in \begin{cases} (\pi, 4] & \text{when } n = 4m : \text{ Quarter-turn symmetry,} \\ (\pi, \frac{9}{2}) & \text{when } n = 4m + 1,\ n = 4m + 3 : \text{ Asymmetric norms,} \\ [3, \pi) & \text{when } n = 4m + 2 : \text{ Radon norms.} \end{cases} \tag{3.11}$$

Corollary 3.3. Combining all three families of polygons, $\pi_n \in [3, \frac{9}{2}]$.

4. Polygons with an offset center

In the following section we analyse the behaviour of π_B for some convex polygons with an offset center. First we consider the general case for a triangle (which has to be isosceles). Then, we analyse the cases for regular squares and hexagons with an offset center.

4.1. **Offset isosceles triangle.** Let's relax the conditions as much as possible and study the half-perimeter of an isosceles triangle using the offset Minkowski functional from definition 2.3. We will denote it π_t.

We refer the interested reader to the Appendix A.2 for the calculations. Given an offset h_2 from the center, the formula for π_t is:

$$\pi_t = \frac{1}{2}\left(\frac{2h}{h_2} + \frac{h}{h - h_2} + \frac{2h}{h_2}\right). \tag{4.1}$$

The derivative with respect to h_2 is: $f'(h_2) = \frac{h}{2(h-h_2)^2} - \frac{2h}{h_2^2}$.

When $\frac{2h}{3} < h_2 < h$, $f'(h_2) > 0$, so π_t increases monotonically with h_2. When $0 < h_2 < \frac{2h}{3}$, $f'(h_2) < 0$, so π_t decreases monotonically with h_2.

Also, when $h_2 \to h$, $\pi_t \to \infty$ and, as we saw before, when $h_2 \to 0$, $\pi_t \to \infty$.

The minimum value for π_t then happens when the derivative is 0 in the interval $0 < h_2 < h$, and can be obtained by substituting $h_2 = \frac{2h}{3}$ in equation (A.26),

$$\pi_t = \frac{1}{2}\left(\frac{2h}{h_2} + \frac{h}{h-h_2} + \frac{2h}{h_2}\right) = \frac{1}{2}\left(3+3+3\right) = \frac{9}{2}, \tag{4.2}$$

and $\frac{a}{r_x} = 3$, $\frac{a}{r} = 3$, and $\frac{b}{x} = 3$. Note that the minimum value does not depend on a, b or any function of both. An example of this case is depicted for a concrete isosceles triangle in Figure 9.

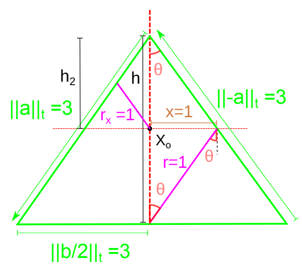

FIGURE 9. Offset isosceles triangle with $\pi_t = 4.5$

We can also calculate, for example, when $\frac{a}{r_x} < \frac{a}{r}$: $\overset{max}{\mu}_t(B_t) = \frac{1}{2}\left(\frac{a}{r} + \frac{a}{r} + \frac{b}{x}\right)$ and $\overset{min}{\mu}_t(B_t) = \frac{1}{2}\left(\frac{a}{r_x} + \frac{a}{r_x} + \frac{b}{x}\right)$.

In this case, if we set $h_2 = \frac{4h}{5}$, $||-a||_t = \frac{a}{r_x} = \frac{2h}{h_2} = \frac{5}{2}$, $||a||_t = \frac{a}{r} = \frac{h}{h-h_2} = 5$, and $||b||_t = \frac{b}{x} = \frac{2h}{h_2} = \frac{5}{2}$, so $\overset{max}{\mu}_t(B_t) = \frac{25}{2}$, $\overset{min}{\mu}_t(B_t) = \frac{15}{2}$, and $\mu_t(B_t) = 10$, so $\pi_t = \frac{\mu_t(B_t)}{2} = \frac{10}{2} = 5$.

Note that both lengths of the side a, $||\vec{a}||_t$ and $||-\vec{a}||_t$ are not the same, as was the case for the centered regular triangle. Moreover, $\overset{max}{\mu}_t(B_t) \neq \overset{min}{\mu}_t(B_t)$.

Watching Figure 9, a general symmetry argument can be made: the minimum happens only when $||\vec{a}||_t = ||-\vec{a}||_t$ and $\overset{max}{\mu}_t(P) = \overset{min}{\mu}_t(P)$, as was the case for the centered regular triangle.

We capture the results of this section in the following observation:

Observation 4.1. *Equation* (4.1) *is symmetric, whether the offset h_2 goes up or down (see Appendix A.2 for more details) the equation is valid. The consequence is that for every value of $\pi_t > 4.5$, every isosceles triangle will have two corresponding center positions, with the same offset with respect to the center (placed in the axis of symmetry, one towards the vertex in the axis of symmetry and one towards its opposite side d and $-d$).*

For polygons with an even number of vertices, there are two possible non equivalent axes of symmetry, one which crosses two vertices and one which goes from the center of one side to the center of the other side. This is depicted in Figure 10.

4.2. **Square with offset center.** Figure 11 depicts the two configurations for a square.

For configuration A: $||l_1||_A = a/h$, $||l_2||_A = 2$, $||l_3||_A = \frac{a}{a-h}$ and $||l_4||_A = 2$.

$$\pi_A = \frac{1}{2}(||l_1||_A + ||l_2||_A + ||l_3||_A + ||l_4||_A) = 2 + \frac{a}{2h} + \frac{a}{2(a-h)}. \tag{4.3}$$

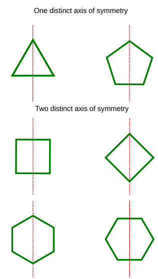

FIGURE 10. Number of non-equivalent axes of symmetry

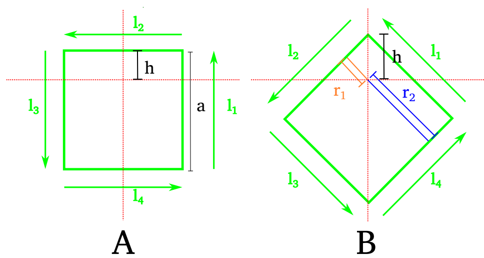

FIGURE 11. Offset square

Taking the derivative: $\frac{d\pi_A}{dh} = -\frac{a}{2h^2} + \frac{a}{2(a-h)^2}$, we can equate it to 0 and: $-\frac{a}{2h^2} + \frac{a}{2(a-h)^2} = 0$, then $h = \frac{a}{2}$. When $h < \frac{a}{2}$, the second term dominates, because $|\frac{a}{2(a-h)^2}| < |\frac{a}{2h^2}|$, so the derivative is negative and $h = \frac{a}{2}$ is a minimum, which gives

$$min_{h=\frac{a}{2}}(\pi_A) = 2 + \frac{2a}{2a} + \frac{a}{2(a - a/2)} = 4. \tag{4.4}$$

For configuration B: By similarity of triangles, $r_1 = \frac{h}{\sqrt{2}}$, so $||l_1||_B = \frac{a}{r_1} = \frac{a\sqrt{2}}{h} = ||l_2||_B$ and $||l_3||_B = \frac{a}{a-r_1} = \frac{a}{a-\frac{h}{\sqrt{2}}} = ||l_4||_B$,

Finally

$$\pi_B = \frac{1}{2}(||l_1||_B + ||l_2||_B + ||l_3||_B + ||l_4||_B) = \frac{a\sqrt{2}}{h} + \frac{a}{a - \frac{h}{\sqrt{2}}}. \tag{4.5}$$

The derivative is: $\frac{d\pi_B}{dh} = -\frac{a\sqrt{2}}{h^2} + \frac{a}{\sqrt{2}(a-\frac{h}{\sqrt{2}})^2}$. This derivative is the same as the one for configuration A but with $h_b = \frac{h}{\sqrt{2}}$, so following the same reasoning, the minimum happens when $h_b = \frac{a}{2} = \frac{h}{\sqrt{2}}$, so $h = \frac{\sqrt{2}a}{2} = \frac{a}{\sqrt{2}}$. Finally,

$$min_{h=\frac{a}{\sqrt{2}}}(\pi_B) = 4. \tag{4.6}$$

Observation 4.2. *Given a value of $\pi_s > 4$, we can find four distinct configurations of the square (two per distinct axis of symmetry) with that value of π_s as half-perimeter.*

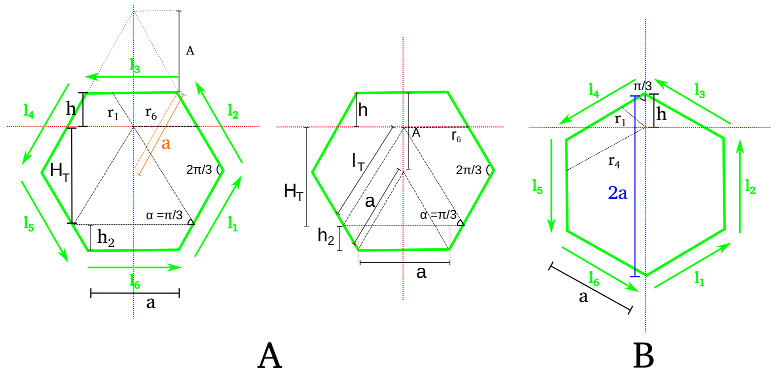

FIGURE 12. Offset hexagon (detail of A)

4.3. **Regular hexagon with offset center.** For the A configuration in Figure 12: The apothem of a regular hexagon, is $A = a\frac{\sqrt{3}}{2}$. We can calculate r_1 by similarity of triangles using Figure 12: $r_1 = a\frac{h}{A} = 2\frac{h}{\sqrt{3}}$.

From triangle similarity of the top triangle, $\frac{A+h}{A} = \frac{r_6}{a/2} = \frac{a\frac{\sqrt{3}}{2}+h}{a\frac{\sqrt{3}}{2}}$, so $r_6 = \frac{a}{2} + \frac{h}{\sqrt{3}}$, $h_2 = 2A - h - H_T$, and $H_T = l_t\frac{\sqrt{3}}{2}$ where l_T is the side of the (equilateral) triangle in the figure. Substituting H_T and A in h_2, $h_2 = a\sqrt{3} - h - l_T\frac{\sqrt{3}}{2}$. From that figure $l_T = 2h_2\frac{cos(\pi/3)}{cos(\pi/6)} + a = \frac{2h_2}{\sqrt{2}} + a$. Substituting h_2, $l_T = 3a - \frac{2h}{\sqrt{3}} - l_T$ so, $l_T = \frac{1}{2}(3a - \frac{2h}{\sqrt{3}})$. Now we can calculate the length of the sides: $||l_1||_A = \frac{a}{r_1} = \frac{a\sqrt{3}}{2h} = ||l_2||_A$, $||l_3||_A = ||l_6||_A = \frac{a}{r_6} = \frac{a}{2\frac{h}{\sqrt{3}}}$ and $||l_5||_A = ||l_4||_A = \frac{a}{l_T} = \frac{2a}{3a-\frac{2h}{\sqrt{3}}}$.

From these, we obtain:

$$\pi_A = \frac{a\sqrt{3}}{2h} + \frac{a}{2\frac{h}{\sqrt{3}}} + \frac{2a}{3a - \frac{2h}{\sqrt{3}}} = \frac{a\sqrt{3}}{h} + \frac{2a}{3a - \frac{2h}{\sqrt{3}}}. \tag{4.7}$$

To find the minimum, we will simplify it with a substitution $H = \frac{2h}{\sqrt{3}}$.

$$\pi_A = \frac{2a}{H} + \frac{2a}{3a - H}. \tag{4.8}$$

With this substitution, we find the derivative:

$$\frac{d\pi_A}{dH} = \frac{-2a}{H^2} + \frac{2a}{(3a-H)^2}. \tag{4.9}$$

The formula for π_A is invalid when $h > \frac{a\sqrt{3}}{2}$, or $H > a$, so we cannot find the minimum by equating the derivative to 0, but for $0 \leq H \leq a$ the second term is dominated by the first $|\frac{2a}{H^2}| \geq |\frac{2a}{(3a-H)^2}|$ so the derivative is negative as H grows, so the minimum is:

$$min_{B=a}(\pi_A) = min_{h=\frac{a\sqrt{3}}{2}}(\pi_A) = 3. \tag{4.10}$$

For the B configuration: Seeing the figure, $r_1 cos(\frac{\pi}{6}) = \frac{h}{2}$, so $r_1 = h$.

Then $||l_1||_B = \frac{a}{r_1} = \frac{a}{h}$, $||l_2||_B = \frac{a}{h}$, $||l_3||_B = ||l_1||_B = \frac{a}{h}$, $||l_4||_B = 1$, $||l_5||_B = \frac{a}{2a-h}$ and $||l_6||_B = ||l_1||_B = ||l_4||_B = 1$, so we obtain:

$$\pi_B = \frac{1}{2}(||l_1||_B + ||l_2||_B + ||l_3||_B + ||l_4||_B) = 1 + \frac{a}{2a-h} + \frac{a}{h}. \tag{4.11}$$

To find the minimum: $\frac{d\pi_B}{dh} = \frac{a}{(2a-\frac{h}{)}^2} - \frac{a}{h^2} = 0$, so $h = a$. We know that $|\frac{a}{(2a-h)^2}| < |\frac{a}{h}|$ when $h < a$ so the derivative is negative and we have found a minimum so:

$$min_{h=a}(\pi_B) = 3. \tag{4.12}$$

Observation 4.3. *Given a value of $\pi_h > 3$, we can find four configurations of the hexagon (two per distinct axis of symmetry), with different positions of the center, with that value of π_h as half-perimeter.*

5. Minimum π_B for the general case

In this section we find the general bounds for π_B for the general case of an asymmetric norm with one axis of symmetry.

First we need the following lemma and some definitions.

Lemma 5.1. *Given $d(y) : \mathbb{R} \to \mathbb{R}$, the width of the unit ball as a function of the displacement y along the axis of symmetry. It will have either a unique point as maximum or an interval. The unique maximum (be it a point or an interval) may be at either ends ($d(y_{max})$ or $d(y_{min})$). If the maximum is not at one end, that end has to be a minimum.*

Proof. The convexity of the unit ball and its axis of symmetry, limits the number of maxima of $d(y)$ to either a unique point or an interval. If there where two separate maxima in $d(y)$, $d(y_1)$ and $d(y_2)$ there would be a minimum between them or $d(y_1) = d(y_2)$, by the extreme value theorem. If there was a minimum between them, then the segment connecting the two maxima would not be completely contained in the unit ball, so it would not be convex. □

From [5], we borrow the following definition:

Definition 5.2. Let $B \subset \mathbb{R}^2$ be a convex set. If $F \subset B$ is non-empty, convex, and $x, y \in B$ and $(x, y) \cap F \neq 0 \Rightarrow x, y \in F$, we call F a *face* of B. We say $p \in B$ is an *extreme point* if $\{p\}$ is a face, i.e. $x, y \in B$ and $p \in (x, y) \Rightarrow x = y = p$. Also from [5] we state (fact (a) after the definition)

Observation 5.3. *If $F \subset B$ is a proper face of B (i.e. $F \neq B$), then $F \subset \partial B$.*

Observation 5.4. *By Lemma 5.1, if we follow the axis of symmetry of a convex set, the two ends are either a face or an extreme point.*

Finally, we are ready to prove the main theorem:

Theorem 5.5. *Given a convex set B with one axis of symmetry, the asymmetric norm defined by* (2.3) *will measure its half-perimeter π_B to be $\pi_B \geq 3$ and π_B can take any value in that range, depending on the concrete norm.*

Proof. In order to find the minimum π_B, we are going to use the construction shown in Figure 14. In that figure x_0 is the center. We displace the unit ball laterally until it touches the center. At either ends following the axis of symmetry, by 5.4 we either have that the end is a face, which can have $\mu(F) \leq d_{x_0}/2$ or an

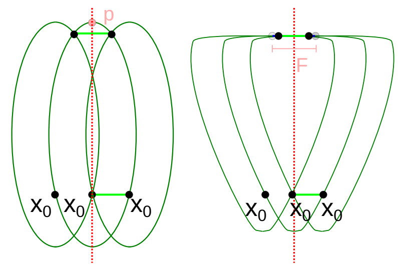

FIGURE 13. Two examples of the construction

extreme point (it is the same case $\mu(F) = 0$) or a face with $\mu(F) > d_{x_0}/2$. For these two cases we have the two behaviours shown in Figure 13. In the first case $\mu(F) \leq d_{x_0}/2$, where the unit ball cuts its copies at the endpoints of a segments of length $d_{x_0}/2$. If not, the length of the segment will be bigger than $d_{x_0}/2$, but the segment will be completely contained in ∂B (because of Observation 5.3), so we can take a subinterval measuring $d_{x_0}/2$ and it will still be contained in ∂B.

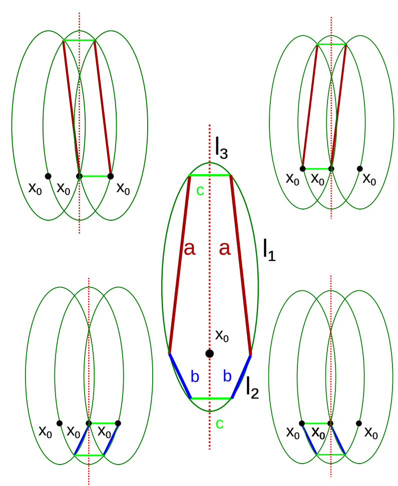

FIGURE 14. Inscribe an hexagon in the unit circle

Using the construction depicted in 14, we can inscribe an hexagon H.

Its sides have Euclidean length $||l_1|| = a$, $||l_2|| = b$, $||l_3|| = c$ and $||-l_3|| = c$, with c, half the diameter at x_0, i.e. $c = d(x_0)/2$. The length given by the Minkowski norm of each side is $||l_1||_B = 1$, $||l_2||_B = 1$, $||l_3||_B = 1$ and $||-l_3||_B = 1$. Note that $||l_1||_B = 1$ and $||l_2||_B = 1$ because the side is $d(x_0)/2$ long and then $||l_3||_B = 1$ (or conversely $||-l_3||_B = 1$), it is a case of parallel transport as depicted in Figure 14.

From Figure 15, we can find the maximum radius of the unit ball for measuring $||-l_1||_B$ and $||-l_2||_B$. Without loss of generality, we assume $a \geq b$. Then, $r_{bmax} = \frac{acos(\beta)}{cos(\alpha+\beta)}$ and $r_{amax} = \frac{bcos(\alpha+\beta)}{cos(\beta)}$. From this: $||-l_1||_B \leq \frac{a}{r_{amax}} = \frac{a\cos(\beta)}{b\cos(\alpha+\beta)}$, $||-l_2||_B \leq \frac{b}{r_{bmax}} = \frac{b\cos(\alpha+\beta)}{a\cos(\beta)}$. We can name $\frac{a\cos(\beta)}{b\cos(\alpha+\beta)} = y$. with $y > 0$. The half-perimeter of the hexagon is then: $\frac{\mu_B(H)}{2} = \frac{||l_1||_B+||-l_1||_B+||l_2|_B+||-l_2||_B+||l_3||_B+||-l_3||_B}{2} \geq$

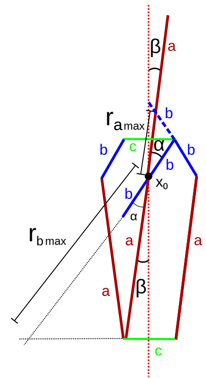

FIGURE 15. Constructions to find r_{bmax} and r_{amax}

$\frac{4+y+\frac{1}{y}}{2}$, so $\frac{\mu_B(H)}{2} \geq 2 + \frac{y+\frac{1}{y}}{2} = f(y)$, This function has an extremum at, $f'(y) = \frac{1-\frac{1}{y^2}}{2} = 0$, so, $y = 1$, and $\frac{\mu_B(H)}{2} = 3$. It is a minimum, because $f''(y) = \frac{1}{y^3} > 0$. From the triangle inequality we have proposition (1.9), so we know that $\pi_B = \frac{1}{2}\mu_B(\partial B) \geq \frac{\mu_B(H)}{2} \geq 3$ and we can conclude that for any asymmetric Minkowski space with an axis of symmetry, the minimum value of π_B, $min(\pi_B) = 3$. From Observation 4.3 we can conclude that π_B takes all the possible values in the range $\pi_B \geq \pi$. □

Acknowledgements

Thanks to Germain Fruteau for may fruitful conversations and computer simulations which have helped this paper immensely.

References

[1] Adler CL, Tanton J. π is the minimum value for Pi. The College Mathematics Journal. 2000;31(2):102-6.
[2] Euler R, Sadek J. The πs go full circle. Mathematics magazine. 1999;72(1):59-63.
[3] Keller JB, Vakil R. π p, the Value of π in l_p. The American Mathematical Monthly. 2009;116(10):931-5.
[4] J C Álvarez Paiva AT. On the perimeter and area of the unit disc. The American Mathematical Monthly. 2005;112(2):141-54.
[5] Sahoo NHB. Extremal Values of Pi. The American Mathematical Monthly. 2022;129(10):933-51.
[6] Thompson AC. Minkowski geometry. vol. 63 of Encyclopedia of Mathematics ands its Applications. Cambridge University Press; 1996.
[7] Martini H, Swanepoel KJ, Weiß G. The geometry of Minkowski spaces—a survey. Part I. Expositiones mathematicae. 2001;19(2):97-142.
[8] Martini H, Swanepoel KJ. The geometry of Minkowski spaces—a survey. Part II. Expositiones mathematicae. 2004;22(2):93-144.
[9] Martini H, Swanepoel KJ. Antinorms and Radon curves. Aequationes mathematicae. 2006;72(1):110-38.
[10] Coxeter HSM. Regular polytopes. New York, NY, USA: Dover Publications; 1973.
[11] Gołab S. Some metric problems of the geometry of Minkowski (Polish French summary). Prace Akademii Górniczej w Krakowie. 1932;6:1-79.
[12] Richter WD, Schicker K. Circle numbers of regular convex polygons. Results in Mathematics. 2016;69:521-38.
[13] Servi LD. Nested square roots of 2. The American Mathematical Monthly. 2003;110(4):326-30.

[14] Beraha S, Kahane J. Is the four-color conjecture almost false? Journal of Combinatorial Theory, Ser B. 1979;27(1):1-12.
[15] Mandal K, Sain D, Paul K. A geometric characterization of polygonal Radon planes. J Convex Anal. 2019;26(4):1113-23.

Appendix A. Appendix

A.1. **Calculations for the regular pentagon .** For the regular pentagon, the apothem $a_5 = \frac{l}{2\tan(\frac{\pi}{5})}$, and $||l||_{\pentagon} = 2 - 2a_5\tan(\frac{\pi}{10}) = 2 - \frac{||l||_{\pentagon}}{\tan(\frac{\pi}{5})}\tan(\frac{\pi}{10})$ so $||l||_{\pentagon} = \frac{2}{1+\frac{\tan(\frac{\pi}{10})}{\tan(\frac{\pi}{5})}} = \frac{(5-\sqrt{5})}{2}$. Finally $\pi_{\pentagon} = \frac{5||l||_{\pentagon}}{2} = \frac{5(5-\sqrt{5})}{4}$.

A.2. **Calculations for the offset isosceles triangle .** Note that π_t is actually a function of the length of the sides and the offset of the center, $\pi_t(a, b, x_o)$. We refer to Figure 16 in this section. We will skip, for the sake of clarity in the following equations the Euclidean norm, so when we denote r we actually mean $||\vec{r}||$ and so on. First,

$$\pi_t = \frac{1}{2}\Big(\frac{a}{r} + \frac{a}{r_x} + \frac{b}{x}\Big). \tag{A.1}$$

We define h as

$$h = h_1 + 2h_2. \tag{A.2}$$

and applying Pythagoras:

$$h = \sqrt{a^2 - \frac{b^2}{4}}. \tag{A.3}$$

We also have

$$\frac{r_2}{2x} = \frac{r_x}{x}, \tag{A.4}$$

$$\frac{x}{h_2} = \tan(\theta) \tag{A.5}$$

and

$$\frac{s}{h_1} = \tan(\theta), \tag{A.6}$$

but also,

$$\frac{\frac{b}{2}}{h} = \frac{b}{2h} = \tan(\theta). \tag{A.7}$$

Also from Pythagoras,

$$s^2 + h_1^2 = r_1^2 \tag{A.8}$$

and

$$x^2 + h_2^2 = r_2^2. \tag{A.9}$$

Note that a and b are the dimensions of the triangle and h_2 set the position of the origin. All the other dimensions depend on these per the equations above.

Combining equations (A.5) and (A.7),

$$\frac{x}{h_2} = \frac{b}{2h},$$

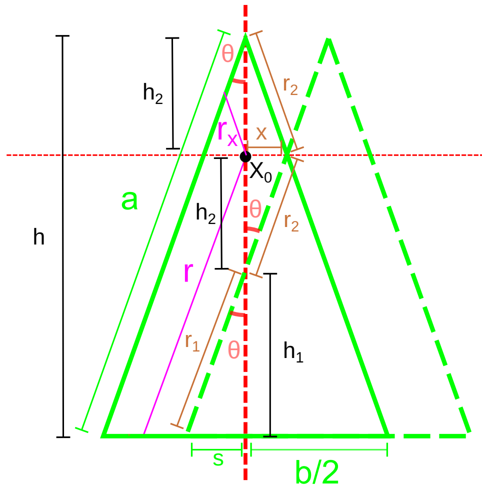

FIGURE 16. Offset isosceles triangle, first configuration

so

$$x = \frac{bh_2}{2h}. \tag{A.10}$$

Similarly, from (A.5) and (A.6),

$$s = \frac{xh_1}{h_2} \tag{A.11}$$

and, from (A.8)

$$\frac{h_1^2 x^2}{h_2^2} + h_1^2 = r_1^2. \tag{A.12}$$

We also have

$$r = r_1 + r_2, \tag{A.13}$$

and from (A.9), combined with (A.12)

$$r = \sqrt{\frac{h_1^2 x^2}{h_2^2} + h_1^2} + \sqrt{h_2^2 + x^2} = h_1 \sqrt{\frac{x^2}{h_2^2} + 1} + \sqrt{h_2^2 + x^2}$$

substituting x from (A.10),

$$r = h_1 \sqrt{\frac{x^2}{h_2^2} + 1} + \sqrt{h_2^2 + \frac{b^2 h_2^2}{4h^2}} = h_1 \sqrt{\frac{b^2}{4h^2} + 1} + h_2 \sqrt{1 + \frac{b^2}{4h^2}},$$

but, from (A.2), $h = h_1 + 2h_2$,

$$r = (h - 2h_2)\sqrt{\frac{b^2}{4h^2} + 1} + h_2 \sqrt{1 + \frac{b^2}{4h^2}} = (h - h_2)\sqrt{\frac{b^2}{4h^2} + 1}. \tag{A.14}$$

Finally, (A.10) and (A.14) and (A.1),

(A.15)

$$\pi_t = \frac{1}{2}\left(\frac{a}{r_x} + \frac{a}{(h - h_2)\sqrt{\frac{b^2}{4h^2} + 1}} + \frac{b}{\frac{bh_2}{2h}} \right) = \frac{1}{2}\left(\frac{a}{r_x} + \frac{a}{(h - h_2)\sqrt{\frac{b^2}{4h^2} + 1}} + \frac{2h}{h_2} \right).$$

We can substitute h, from (A.3),

$$\pi_t = \frac{a}{2r_x} + \frac{a}{2(\sqrt{a^2-\frac{b^2}{4}}-h_2)\sqrt{\frac{b^2}{4(a^2-\frac{b^2}{4})}+1}} + \frac{\sqrt{a^2-\frac{b^2}{4}}}{h_2}.$$

But, from (A.4), $r_x = \frac{r_2}{2}$ and from (A.9) $r_2 = \sqrt{x^2-h_2^2}$, so

$$r_x = \frac{\sqrt{x^2-h_2^2}}{2} = \frac{\sqrt{\frac{(bh_2)^2}{4h^2}-h_2^2}}{2} = \frac{1}{4}\sqrt{\frac{(bh_2)^2}{h^2}-4h_2^2} = \frac{h_2}{4}\sqrt{\frac{b^2}{h^2}-4},$$

substituting in r_x and h, from (A.3),

$$\pi_t = \frac{2a}{h_2\sqrt{\frac{b^2}{a^2-\frac{b^2}{4}}-4}} + \frac{a}{2(\sqrt{a^2-\frac{b^2}{4}}-h_2)\sqrt{\frac{b^2}{4(a^2-\frac{b^2}{4})}+1}} + \frac{\sqrt{a^2-\frac{b^2}{4}}}{h_2},$$

$$\pi_t = \frac{1}{h_2\sqrt{\frac{1}{a^2-\frac{b^2}{4}}}} + \frac{a}{2(\sqrt{a^2-\frac{b^2}{4}}-h_2)\frac{a}{\sqrt{a^2-\frac{b^2}{4}}}} + \frac{\sqrt{a^2-\frac{b^2}{4}}}{h_2},$$

substituting back h, from (A.3),

$$\pi_t = \frac{h}{h_2} + \frac{a}{2(h-h_2)\frac{a}{h}} + \frac{h}{h_2},$$

so we obtain

$$\pi_t = \frac{h}{h_2} + \frac{h}{2(h-h_2)} + \frac{h}{h_2}. \tag{A.16}$$

Note that π_t is not bounded. When $h_2 \to 0$, $\pi_t \to \infty$.

The other end, cannot be represented with this construction, because h_1 would be negative.

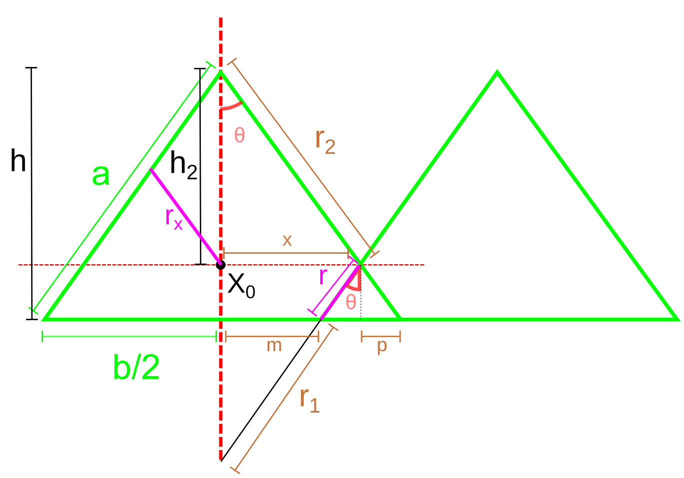

FIGURE 17. Offset isosceles triangle, second configuration

We show the second configuration, in Figure 17. In this configuration, the next are true:

$$\frac{h-h_2}{p} = \frac{h_2}{x}, \tag{A.17}$$

$$\frac{r_2}{2x} = \frac{r_x}{x}, \tag{A.18}$$

$$r_1 + r = r_2, \tag{A.19}$$

$$r_2 = a - r, \tag{A.20}$$

and, from Pythagoras,

$$r^2 = p^2 + (h-h_2)^2, \tag{A.21}$$

$$h = \sqrt{a^2 - \frac{b^2}{4}}, \tag{A.22}$$

and,

$$r_2^2 = x^2 + h_2^2. \tag{A.23}$$

From (A.21) and (A.20),

$$x = \sqrt{(a-r)^2 - h_2^2} \tag{A.24}$$

Combining (A.21), (A.24) and (A.17),

$$r^2 = \frac{x^2(h-h_2)^2}{h_2^2} + (h-h_2)^2 = \frac{x^2(h-h_2)^2}{h_2^2} + (h-h_2)^2,$$

and, substituting (A.24),

$$r^2 - \frac{(h-h_2)^2(a-r)^2}{h_2^2} = 0,$$

and expanding the right side,

$$r^2\Big(\frac{h_2^2}{(h-h_2)^2} - 1\Big) + 2ar - a^2 = 0.$$

Solving the quadratic equation for r,

$$r = \frac{-2a \pm \sqrt{4a^2 + 4a^2(\frac{h_2^2}{(h-h_2)^2} - 1)}}{a\Big(\frac{h_2^2}{(h-h_2)^2} - 1\Big)} = \frac{a(-1 \pm \frac{h_2}{h-h_2})}{\frac{h_2^2}{(h-h_2)^2} - 1}.$$

Note that $r > 0$ and $h - h_2 < h_2$, so $\frac{h_2^2}{(h-h_2)^2} > 1$, so we can discard the negative solution above we introduced when we squared r:

$$r = \frac{a(-1 + \frac{h_2}{h-h_2})}{\frac{h_2^2}{(h-h_2)^2} - 1} = \frac{a}{1 + \frac{h_2}{h-h_2}}. \tag{A.25}$$

$$\pi_t = \frac{1}{2}\Big(\frac{a}{r_x} + \frac{a}{r} + \frac{b}{x}\Big),$$

substituting r from (A.24) and x from (A.25),

$$\pi_t = \frac{1}{2}\left(\frac{a}{r_x} + \frac{h}{h-h_2} + \frac{b}{h_2\sqrt{\left(\frac{a}{h}\right)^2 - 1}}\right).$$

substituting (A.22),

$$\pi_t = \frac{1}{2}\left(\frac{a}{r_x} + \frac{h}{\sqrt{a^2 - \frac{b^2}{4}} - h_2} + \frac{2}{h_2\sqrt{\frac{1}{a^2 - \frac{b^2}{4}}}}\right).$$

Combining (A.18) and (A.20), we get $r_x = \frac{r_2}{2} = \frac{a-r}{2}$, so

$$\pi_t = \frac{1}{2}\left(\frac{2a}{a - \frac{a}{1+\frac{h_2}{h-h_2}}} + \frac{h}{\sqrt{a^2 - \frac{b^2}{4}} - h_2} + \frac{2}{h_2\sqrt{\frac{1}{a^2 - \frac{b^2}{4}}}}\right)$$

substituting (A.22) back,

$$\pi_t = \frac{1}{2}\left(\frac{2h}{h_2} + \frac{h}{h-h_2} + \frac{2h}{h_2}\right). \tag{A.26}$$

Note that (A.26) is the same as (A.16). In both equations, h_2 and h represent the same dimensions (the height of the triangle and the offset from its highest point to the chosen center respectively) so we can analyze both simultaneously using the same equation.

Rey Juan Carlos University, Madrid, Spain
Email address: gorka.guardiola@urjc.es